Preparation of Large-Scale Double-Side BDD Electrodes and Their Electrochemical Performances

Wu Haibing(吴海兵), *Xu Feng*(徐锋)*, *Liu Zhaozhi*(刘召志), *Zhou Chun*(周春), *Lu Wenzhuang*(卢文壮), *Zuo Dunwen*(左敦稳)

College of Mechanical and Electrical Engineering, Nanjing University of Aeronautics and Astronautics, Nanjing 210016, P. R. China

(Received 4 November 2014; revised 24 June 2015; accepted 25 October 2015)

Abstract: Boron doped diamond (BDD) performs well in electrochemical oxidation for organic pollutants thanks to its wide electrochemical window and superior chemical stability. We presented a method to obtain well-adherent large-scale BDD/Nb electrode by the modified hot filament chemical vapor deposition system (HFCVD). SiC particles were sand blasted to enhance the adhesion of BDD coating. The BDD coating was then deposited on both sides of Nb which was placed vertically and closely with filament grids on both sides. The BDD/Nb electrodes had no deformation because the thermal deformations of the BDD films on both sides of the Nb substrate conteracted each other during cooling process after deposition. The surface morphology and purity of the BDD/Nb electrode were analyzed by Raman and scanning elestron microscope (SEM) techniques. Scratch test was used to investigate the adhesion of BDD films. The electrochemical performances were measured by cyclic voltammetry test. The BDD electrode at the B/C ratio of $2\ 000\times10^{-6}$ held a higher oxygen evolution potential thanks to its high sp3 carbon content. Accelerated life test illustrated that the sandblasting pretreatment obviously enhanced the adhesion of BDD coating which resulted in a longer service duration than the un-sandblasted one.

Key words: hot filament chemical vapor deposition (CVD); boron doped diamond; large-scale double side electrode; electrochemical performances

CLC number: TB43 **Document code**: A **Article ID**: 1005-1120(2015)06-0674-07

0 Introduction

Conductive boron doped diamond (BDD) has outstandingly electrochemical performance thanks to its wide potential window, high oxygen evolution potential, low background current, and superior chemical and dimensional stability[1-3]. Thus, BDD has been an excellent electrode material for electrochemical oxidation for organic pollutant in wastewater. And there is no any other kind of electrodes can compete.

At present, BDD is normally deposited with microwave plasma chemical vapor deposition (MPCVD)[4-5] and hot filament chemical vapor deposition (HFCVD)[6-7] techniques. HFCVD is a promising method for industrial fabrication of BDD electrodes because of its low cost, simplicity of required apparatus, and the ability to deposit large-scale diamond films[8]. Current researches have mostly focused on the preparation of single-side BDD electrode using traditional HFCVD system. The substrate and tungsten filaments are horizontally laid out in the HFCVD vacuum chamber. Si, Ti and Nb are the commonly used substrate for BDD growth. They can form carbides at the interface between the substrate and the diamond coating. Si is not adapted for large-scale electrode preparation due to its brittleness[9]. The use of metal substrate materials is highly desirable for electrochemical applications

* **Corresponding author**: Xu Feng, Professor, E-mail: xufeng@nuaa.edu.cn.

How to cite this article: Wu Haibing, Xu Feng, Liu Zhaozhi, et al. Preparation of large-scale double-side BDD electrodes and their electrochemical performances[J]. Trans. Nanjing U. Aero. Astro., 2015,32(6):674-680.
http://dx.doi.org/10.16356/j.1005-1120.2015.06.674

because of the enhanced electrical conductivity and the increased substrate area. However, the thermal expansion coefficients of the substrate materials are different from those of diamond. After deposition, the thermal stress is caused by the mismatch of thermal expansion between diamond films and the substrate during the substrate cooling down from high temperature to room temperature. Thermal stress results in thermal deformation, especially in the fabrication of large-scale electrodes. Our previous research results indicated that deformation of large-scale BBD electrode frequently occurred in the deposition of single side BDD electrode using traditional HFCVD system. This kind of deformation strongly affects the adhesion stability of BDD electrode and consequently influences its industrial applications.

We present a method to prepare the large-scale double-side BDD electrode in a modified HFCVD system to prevent thermal deformation of BDD electrode. Diamond coating has low adhesion on Ti substrate because the formation of TiC and TiH_2 has already generated loose structure before diamond nucleation and growth in the CVD atmosphere[10-11]. Our previous work showed that Nb substrate was fit for the chemical vapor deposition (CVD) diamond growth with good adhesion between diamond films and Nb[12]. Therefore, Nb is selected as the substrate for BDD deposition.

After deposition, the thermal deformation generated from both sides of BDD electrode can thus counteract each other during the cooling process from the high substrate temperature of nearly 800 °C. Moreover, the double-side BDD electrode is supurior to the single-side BDD because BDD coating on both side of one electrode actually works as two cathodes. The double-side electrode has higher treating efficiency than single-side one and consequently reduces the use of expensive Nb substrate materials. Therefore, we prepare the well-adherent BDD coating on Nb substrate and study their electrochemical performances. The accelerated life test is used to investigate the stability of BDD electrode.

1 Experiment

The BDD films were deposited on the Nb substrate in a modified HFCVD system, as shown in Fig. 1. Two tungsten filament grids were parallelly arranged at both sides of the vertically placed substrate. The distance between substrate and filaments was about 10 mm, the same as the filament intervals.

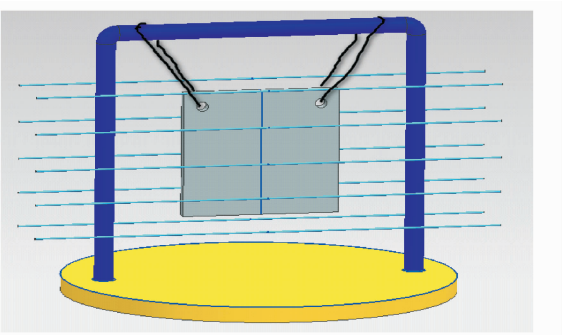

Fig. 1 Arrangements of filaments and Nb substrate for double-side BDD deposition

The deposition of BDD was performed in a gas mixture of CH_4, H_2, and B_2H_6 at a total gas flow rate of 400 sccm and a total gas pressure of 2.5 kPa. The B_2H_6 was diluted by H_2 to 1 vol %. The carbon concentration was maintained by carbon to hydrogen ration (C/H) of 1% and the boron concentration was adjusted by boron to carbon ratio (B/C) varying from $2\,000\times10^{-6}$ to $10\,000\times10^{-6}$. The tungsten filament temperature was whin the range of 2 600—2 700 ℃ and the substrate temperature was about (790 ± 10) ℃ measured with a K-type thermocouple.

50 mm × 100 mm × 2 mm Nb plates were used as the substrates. The small size substrates were used to reveal the effects of boron doping on composition and microstructure of BDD films. Before deposition, SiC particles were sand blasted to coarsen the substrate surface therefore to enhance the nucleation and the adhesion of the coating on the substrate. Then, the substrates were ultrasonically cleaned in 5 M HCl solution for

30 min and successively deionized in water for 5 min.

The phase composition of the BDD films was characterized by RENISHAW Raman spectroscopy. The laser source was emitted from argon ions with a wavelength of 514.5 nm. The surface morphology was determined using Hitachi S4800 SEM system. The adhesion tests were carried out by a wear test conducted with BDD coating in contact with a Si_3N_4 ball at a pin-disc-type wear testing apparatus. The resistivity of the BDD samples was detected by a 4-pin probe method[13]. Cyclic voltammetric behavior was observed by 0.5 M H_2SO_4 solution with a standard three-electrode. Pt wire was used as a counter-electrode, and calomel electrode as a reference electrode. The accelerated life tests of BDD/Nb electrode were conducted in 3 M H_2SO_4 solution at the temperature of 50 ℃ under a current density of 1 A/cm^2[14]. The potential of the working electrode was periodically monitored under the constant current source mode.

2 Result and Discussion

Fig. 2(a) shows the front view of the double-side BDD sample, where homogeneous BDD films are looked as uniform coverage of the deep dark color on the substrate which means they were deposited on the Nb substrate. The side views of the single-side BDD sample and the double-side one are compared in Fig. 2(b). The double-side sample has nearly no bending while the single-side one has an obvious bending deformation. The thermal stress emerged during the cooling process due to the thermal mismatch between the diamond and the substrate. At the situation of the single-side electrode, the thermal stress resulted in the elastic bending toward the substrate side, which could be explained by the Stoney equation[15]. But at the case of double-side electrode, the equal and opposite thermal bending deformations were produced at the both side of substrate, so the total bending deformation was thus zero, resulting in the flat double-side large area electrode.

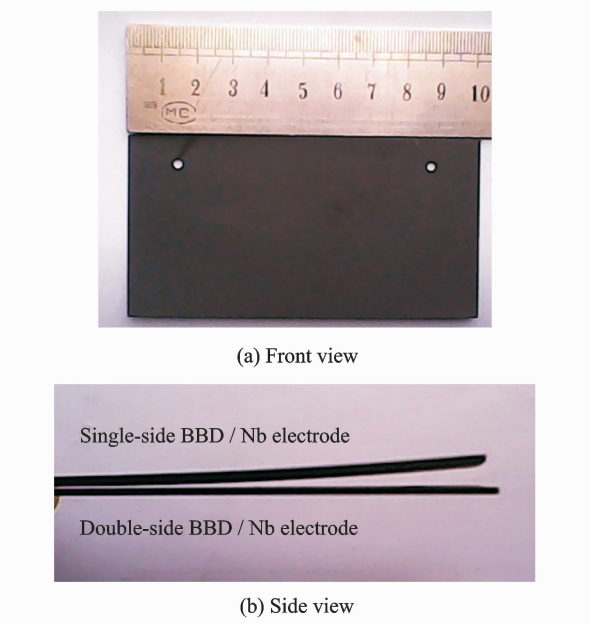

Fig. 2 Optical pictures of the as-prepared BDD electrodes

Fig. 3 shows the Raman spectra of the BDD films grow at different B/C ratios varying from $2\,000\times10^{-6}$ to $10\,000\times10^{-6}$. At the low B/C ratio of $2\,000\times10^{-6}$, curve a in Fig. 3, a sharp diamond peak located at 1 332 cm^{-1} and a broad graphite (G) peak centered at 1 580 cm^{-1}, which denote the high quality of diamond grains and the inclusion of a small amount of sp^2 carbon. The broad peaks at 500 and 1 220 cm^{-1} are also observed in curve a, due to Fano interference effect as a result of boron doping in diamond films[16]. The diamond peak position shifted from 1 332 to 1 305 cm^{-1} with increasing B/C ratio from $2\,000\times10^{-6}$ to $10\,000\times10^{-6}$. The red shift of diamond peak was related to the Fano effects caused by boron doping and tensile residual stress in the films[17-18]. Curves a—d show the intensity of diamond peak at about 1 332 cm^{-1} decreases and that of graphite peak at about 1 550—1 580 cm^{-1} increases with the increase of boron doping concentration. The graphite (D) peak at 1 350 cm^{-1} was observed obviously at the heavy level boron doping of $10\,000\times10^{-6}$. The results revealed that the boron doping causes the decrease of diamond purity.

Fig. 4 shows the SEM images of the BDD

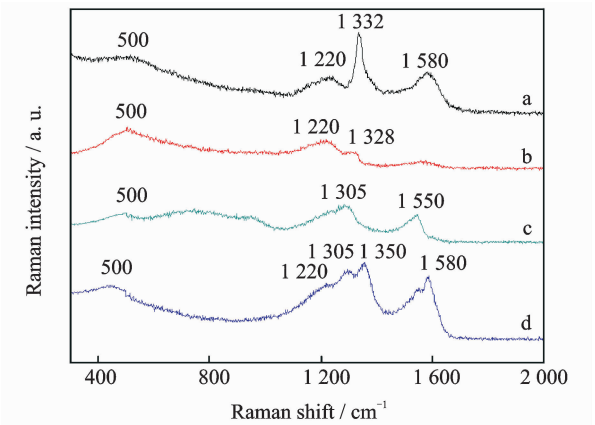

a: 2 000×10^{-6}, b: 4 000×10^{-6}, c: 8 000×10^{-6}, d:10 000×10^{-6}

Fig. 3 Raman spectra of the BDD samples at different B/C ratios

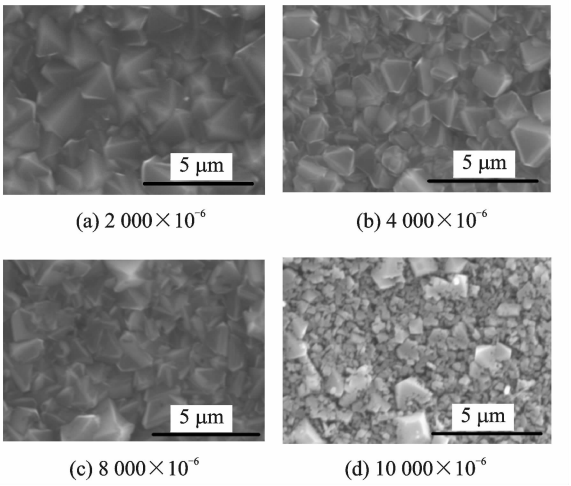

Fig. 4 SEM images of BDD films prepared at different B/C ratios

samples deposited at B/C ratios of 2 000×10^{-6}, 4 000×10^{-6}, 8 000×10^{-6}, and 10 000×10^{-6}. At the low doping level of 2 000×10^{-6}, the BDD films were composed of faceted diamond grains. The grain size of diamond decreased from 4 to 2 μm as the B/C ratio increasing from 2 000×10^{-6} to 8 000×10^{-6}. Well faceted diamond crystallites were gradually degenerated as well as the density of secondary nucleation increased as the increase of B/C ratio. At the heavy boron doping level of 10 000×10^{-6}, the grain size of diamond turned smaller evidently and the grains appeared in incomplete shapes with unclear boundaries. The secondary nucleation of diamond brought lots of sp^2 non-diamond contents, which was also confirmed by the Raman results.

The wear test was used to investigate the adhesion of BDD coating on the substrate. The wear scar on the films was determined comprehensively by the coating-substrate adhesion and the coating hardness. The pictures of the wear scar of the samples pretreated with and without sandblasting treatment are shown in Figs. 5(a, b), respectively. The coating on the substrate without sandblasting treatment was peeled off from the substrate and the metallic substrate can be found after wear test of 0.5 h, as shown in Fig. 5(a). While the coating on the substrate with sandblasting only showed a slight wear vestige after the wear test for 1 h. The typical morphology of wear surface of the BDD films can be found in the Fig. 5(c). Its energy dispersive spectrometer (EDS) result is shown in Fig. 5(d). Thanks to the good adhesion ability of the BDD films on the sandblasting pretreated Nb substrate, only slight chafing can be found in Fig. 5(c), and the electrode surface is fully covered with BBD films as only carbon element can be detected in Fig. 5(d).

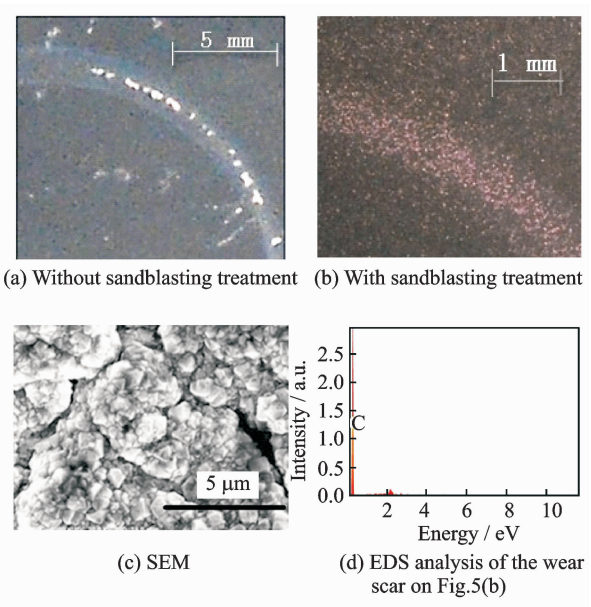

Fig. 5 BDD coatings after wear test prepared on the Nb substrate

The above results indicat that sandblasting pretreatment can enhance the adhesion of BDD coating on the Nb substrate. The substrate

surface roughness was measured by profilometer with and without sandblasting pretreatment before BDD deposition, which were Ra 1.2 μm and Ra 0.17 μm, respectively. Moreover, lots of craters with sharp edges were produced in the substrate surface after sandblasting SiC particles. The improvement of coating-substrate adhesion was related to diamond nucleation enhancement at the rough sandblasted substrate surface. The micro crater edge sites on the highly disordered sandblasted surface created high energy sites, which were the preferred diamond nucleation sites as its minimization of interfacial energy by the formation of diamond nuclei[19]. The most rapid carbon saturation occurred at the sharp edge of micro craters on the strong carbon forming metal substrate, which was also an important reason for the diamond nucleation enhancement.

Table 1 shows the influence of B/C ratio on the resistivity and electrochemical properties of BDD samples. The undoped diamond displays the character of insulator materials. The resistivity of the BDD sample is about 5×10^{-3} Ω·cm at B/C ratio of $2\ 000\times10^{-6}$. Its resistivity drops as the increase of boron doping level. The electrochemical window is broader than other electrode materials especially in the low boron doping level. The potential for oxygen evolution is about 2.3 V at B/C ratio of $2\ 000\times10^{-6}$. Most organic materials have the oxidation potentials in the range of 1.5—2.0 V. Therefore, most of the organics can be oxidized and decomposed at the BDD electrode[20]. The oxygen evolution potential and hydrogen evolution potential get slowly close to 0 V with the increasing boron doping level, which causes the gradual narrowing of the electrochemical potential window of the BDD electrode. Also the background currents and peak currents on the anode and cathode increase with the increase of boron doping level, because of the increase of non-diamond sp^2 carbon in the BDD coating[21]. The cyclic voltammetric curves of the BDD samples deposited at B/C ratio of $10\ 000\times10^{-6}$ can not be obtained as its low sp^3 carbon content and low adhesion of the coating and the substrate. In our HFCVD system, the B/C ratio of $2\ 000\times10^{-6}$ is the proper boron doping level as its appropriate electrical resistivity, wide potential window and high oxygen evolution potential. The choice of boron doping level should keep the high sp^3 content while obtaining a proper electrical resistivity.

Table 1 Effect of boron doping level on the electrochemical properties of the BDD/Nb electrodes

B doping level/10^{-6}	Resistivity/(Ω·cm)	Potential for hydrogen evolution/V	Potential for oxygen evolution/V	Background currents/A	Potential window/V	Cathodic peak currents/A	Anodic peak currents/A
2 000	5×10^{-3}	−1.1	2.3	$\pm2\times10^{-5}$	3.4	−0.05	0.05
4 000	2×10^{-3}	−1.0	2.3	$\pm1\times10^{-4}$	3.3	−0.04	0.03
8 000	1×10^{-3}	−0.7	1.8	$\pm2\times10^{-4}$	2.5	−0.38	0.10
10 000	0.8×10^{-3}						

Fig. 6 reports the accelerated test results of Nb/BDD electrodes pretreated with and without SiC particle sandblasting deposited at B/C ratio of $2\ 000\times10^{-6}$. The BDD electrode held a long-term stability in the accelerated test. They worked at a stable state for long time in the solution of 3 M H_2SO_4 aqueous at the current density of 1 A/cm^2. The service lifetimes of the BDD electrodes with and without sandblasting pretreatment are 170 and 90 h, respectively. The electrode with sandblasting pretreatment held longer service duration than the un-sandblasted one. At last the voltage of BDD electrode increased drastically and the electrode lost its work ability as the BDD coating adhesion were deteriorated obviously. The normal working parameters in wastewater treatment are usually much lower than the accelerated test. Therefore, the real service lifetime of the BDD electrode should be much longer under the normal parameters.

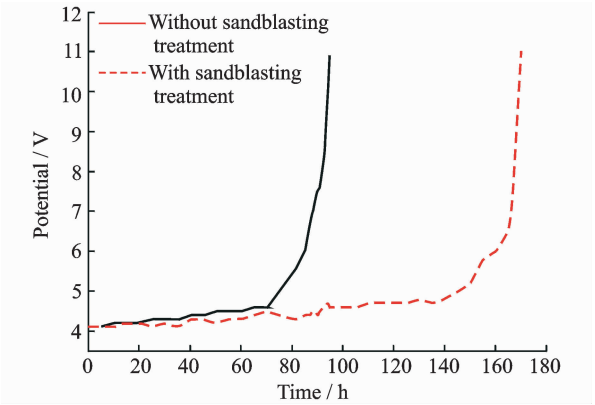

Fig. 6 Accelerated life of the BDD films on the substrates

The service lifetime of the electrode is related to the adhesion of the substrate and diamond coating. Figs. 7(a, b) show the SEM images of the surface morphology of the BDD electrode sample with sandblasting treatment after 30 and 160 h of accelerated life test. At the initial stage of accelerated life test, the surface morphology of BDD was similar to the as-deposit diamond film. Lots of the micro pits and defects could be found with columnar growth mode of CVD diamond. At the last stage of life test, large area of diamond film peeled off the substrate, as shown in Fig. 7(b). Large area detachment of diamond film could also be found in the sample without sandblasting treatment at the working time of 90 h when it lost its working ability in the accelerated life test. The faults in the diamond were destroyed by the generated bubbles or current load in the corrosive solution. Then the aqueous solution permeated into the interface of the substrate and the coating and diffused along the interface, which caused the coating peel off the substrate and electrode inactivation. Therefore, the inactive mechanism of BDD electrode is the detachment of diamond film from Nb substrate. The adhesion of the coating and substrate will determine the working life of the BDD electrode. The BDD electrode with blasting treatment has longer service lifetime because it has better adhesion of the substrate and coating. Therefore, further measures can improve the adhesion of diamond film for longer service lifetime of BDD electrode in the future.

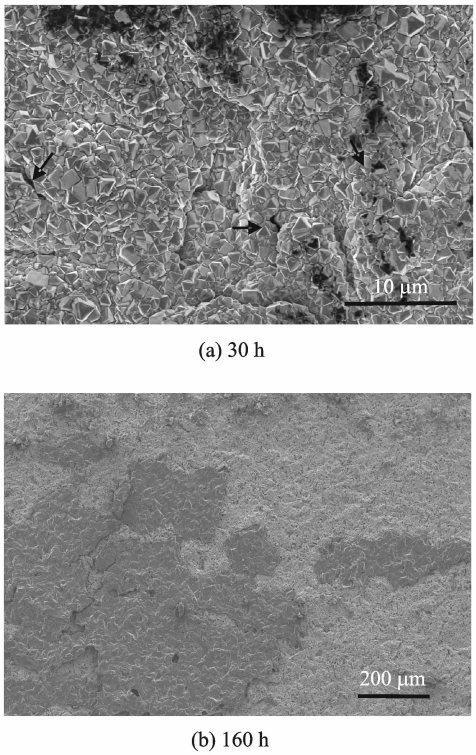

(a) 30 h

(b) 160 h

Fig. 7 SEM of BDD film surface morphology after 30 and 160 h of accelerated life test

3 Conclusions

We presented a method to prepare the large-scale double-side boron doped diamond electrode without thermal deformation in the modified HF-CVD system. The total thermal deformation of the BDD electrode was zero because of the counteraction of the thermal deformations generated between the BDD coatings on both sides. The B/C ratio of $2\,000\times10^{-6}$ is the optimized boron doping level as its proper electrical resistivity, wide potential window and high oxygen evolution potential. High boron doping level will lead to the poor diamond quality and poor electrochemical performances. The sandblasting with SiC particles pretreatment can obviously enhance the adhesion of BDD/Nb electrode, resulting in the longer service duration.

Acknowledgements

This work was supported by the National Natural Science Foundation of China (Nos. 51575269, 51275232), the

Six Talent Peaks Project in Jiangsu Province (No. ZBZZ-005), and the Zhejiang Provincial Key Laboratory for Cutting Tools (No. ZD201305).

References:

[1] Panizza M, Cerisola G. Application of diamond electrodes to electrochemical processes[J]. Electrochimica Acta, 2005,51(2):191-199.

[2] Wei J J, Li C M, Gao X H, et al. The influence of boron doping level on quality and stability of diamond film on Ti substrate[J]. Applied Surface Science, 2012,258(18):6909-6913.

[3] Yano T, Popa E, Tryk D A, et al. Electrochemical behavior of highly conductive boron-doped diamond electrodes for oxygen reduction in acid solution[J]. Journal of the Electrochemical Society, 1999, 146 (3):1081-1087.

[4] Ramamurti R, Becker M, Schuelke T, et al. Boron doped diamond deposited by microwave plasma-assisted CVD at low and high pressures[J]. Diamond and Related Materials, 2008,17(4/5):481-485.

[5] Zou Y S, Li Z X, Yang H. Microstructure and field electron emission properties of boron doped diamond films[J]. Surface Engineering, 2011, 27 (4): 294-299.

[6] Jia F C, Bai Y Z, Qu F, et al. The influence of gas pressure and bias current on the crystallinity of highly boron-doped diamond films[J]. New Carbon Materials, 2010,25(5):357-361.

[7] Doi T, Fukaishi T, Hiramatsu C, et al. Effectiveness of a hot-filament chemical vapor deposition method for preparation of a boron-doped superconducting diamond film with higher superconducting transition temperature[J]. Diamond and Related Materials, 2012,25(5):5-7.

[8] Xu F, Zuo D W, Lu W Z, et al. Microstructure and residual stress in nanocrystalline diamond film[J]. Acta Metallurica Sinica, 2008,44(1):74-78.

[9] Zhang T, Zhang J G, Shen B, et al. Simulation of temperature and gas density field distribution in diamond films growth on silicon wafer by hot filament CVD[J]. Journal of Crystal Growth, 2012,343 (1): 55-61.

[10] Panizza M, Cerisola G. Application of diamond electrodes to electrochemical processes[J]. Electrochimica Acta, 2005,51(2):191-199.

[11] Gerger I, Haubner R. The behaviour of Ti-substrates during deposition of boron doped diamond[J]. International Journal of Refractory Metals and Hard Materials, 2008,26(5):438-443.

[12] Xu F, Xu J H, Yuan M F, et al. Adhesion improvement of diamond coatings on cemented carbide with high cobalt content using PVD interlayer[J]. Diamond and Related Materials, 2013,34(4):70-75.

[13] Petherbridge J R, May P W, Fuge G M, et al. In situ plasma diagnostics of the chemistry behind sulfur doping of CVD diamond films[J]. Diamond and Related Materials, 2002,11(3/4/5/6): 301-306.

[14] Chen X M, Gao F R, Chen G H. Comparison of Ti/BDD and Ti/SnO_2-Sb_2O_5 electrodes for pollutant oxidation[J]. Journal of Applied Electrochemistry, 2005,35(2):185-191.

[15] Peng X L, Tsui Y C, Clyne T W. Stiffness, residual stresses and interfacial fracture energy of diamond films on titanium[J]. Diamond and Related Materials, 1997,6(11):1612-1621.

[16] Wang Y G, Lau S P, Tay B K, et al. Resonant Raman scattering studies of Fano-type interference in boron doped diamond[J]. Journal of Applied Physics, 2002,92(12):7253-7256.

[17] Ferreira N G, Abramof E, Corat E J, et al. Residual stresses and crystalline quality of heavily boron-doped diamond films analysed by micro-Raman spectroscopy and X-ray diffraction[J]. Carbon, 2003,41(6): 1301-1308.

[18] Li H D, Zhang T, Li L, et al. Investigation on crystalline structure, boron distribution, and residual stresses in freestanding boron-doped CVD diamond films[J]. Journal of Crystal Growth, 2010,312(12/13):1986-1991.

[19] Liu H M, Dandy D S. Diamond chemical vapor deposition: Nucleation and early growth stages[M]. Michigan: Noyes Publications, 1995:111-130.

[20] Rodrigo M A, Canizares P, Sanchez-Carretero A, et al. Use of conductive-diamond electrochemical oxidation for wastewater treatment[J]. Catalysis Today, 2010,151(1/2):173-177.

[21] Gerger I, Haubner R, Kronberger H, et al. Investigation of diamond coatings on titanium substrates for electrochemical applications[J]. Diamond and Related Materials, 2004,13(4/5/6/7/8):1062-1069.

(Executive Editor: Zhang Bei)